Fermi surface of a system with strong valence fluctuations: Evidence for a noninteger count of valence electrons in EuIr2Si2

K. Götze, B. Bergk, O. Ignatchik, A. Polyakov, I. Kraft, V. Lorenz, H. Rosner, T. Förster, S. Seiro, Ilya Sheikin, et al.

Fermi Surface of a System with Strong Valence Fluctuations: Evidence for a Non-Integer Count of Valence Electrons in $EuIr_2Si_2$

K. Götze,[1,2,*] B. Bergk,[1,3] O. Ignatchik,[1] A. Polyakov,[1] I. Kraft,[4,5] V. Lorenz,[6] H. Rosner,[4] T. Förster,[1] S. Seiro,[4,6] I. Sheikin,[7] J. Wosnitza,[1,5] and C. Geibel[4,†]

[1] *Hochfeld-Magnetlabor Dresden (HLD-EMFL) and Würzburg-Dresden Cluster of Excellence ct.qmat, Helmholtz-Zentrum Dresden-Rossendorf, 01328 Dresden, Germany*

[2] *Department of Physics, University of Warwick, Coventry, CV4 7AL, United Kingdom*

[3] *Institut für Werkstoffwissenschaft, TU Dresden, 01062 Dresden, Germany*

[4] *Max Planck Institute for Chemical Physics of Solids, 01187 Dresden, Germany*

[5] *Institut für Festkörper- und Materialphysik, Technische Universität Dresden, 01062 Dresden, Germany*

[6] *Leibniz IFW Dresden, 01069 Dresden, Germany*

[7] *Laboratoire National des Champs Magnétiques Intenses (LNCMI-EMFL), CNRS, UGA, 38042 Grenoble, France*

(Dated: March 24, 2022)

We present de Haas-van Alphen (dHvA) measurements on a Eu-based valence-fluctuating system. $EuIr_2Si_2$ exhibits a temperature dependent, non-integer europium valence with $Eu^{2.8+}$ at low temperatures. The comparison of experimental results from our magnetic-torque experiments in fields up to 32 T and density functional theory band-structure calculations with localized $4f$ electrons shows that the best agreement is reached for a Fermi surface based on a valence of $Eu^{2.8+}$. The calculated quantum-oscillations frequencies for Eu^{3+} instead cannot explain all the experimentally observed frequencies. The effective masses, derived from the temperature dependence of the dHvA oscillation amplitudes, show not only a significant enhancement with masses up to 11 m_e (m_e being the free electron mass), but also a magnetic-field dependence of the heaviest mass. We attribute the formation of these heavy masses to strong correlation effects resulting from valence fluctuations of $4f$ electrons being strongly hybridized with conduction electrons. The increase of the heavy masses with magnetic field likely results from the onset of the expected field-induced valence crossover that enhances these valence fluctuations but does not alter the Fermi-surface topology in the field range studied.

I. INTRODUCTION

Having knowledge of the electronic structure at and in the vicinity of the Fermi level allows to predict and understand important physical properties of a material. How correlations modify the electronic structure around the Fermi level, and, in particular, the Fermi surface (FS), is a fundamental problem of condensed-matter physics. Much effort has been devoted to its investigation in materials such as superconducting high-T_c cuprates [1–3] and heavy-fermion compounds based on Ce and Yb [4–12].

In the latter compounds, the $4f$ electron (Ce) or $4f$ hole (Yb) can evolve from a fully localized state to a fully itinerant one depending on its interaction with conduction electrons. A yet only partially resolved question is under which condition the $4f$ electron is included into the Fermi volume [5]. Depending on the answer, the number of electrons in the Fermi volume shall differ, resulting in very different FSs. In contrast, in weakly correlated materials the number of electrons in the Fermi volume is well determined by the number of valence electrons, and hence the FS, too. A further notable difference between heavy-fermion systems and weakly correlated ones is the effective mass of the quasiparticles forming the FS. Whereas in weakly correlated compounds the enhancement of the effective mass due to correlations is small, typically well below a factor of 2, in heavy-fermion systems the enhancement factor can reach values of several hundreds, hence the name heavy-fermion systems [4, 13].

The size of the Fermi volume and the FS in strongly correlated systems is connected with a fundamental problem in theoretical physics: the validity of Luttinger's theorem [14]. Luttinger's theorem is a major result in many-body physics that states the volume of the FS is directly proportional to the particle density. In its hard form, it implies that the Fermi volume is invariant with respect to interactions [15]. Ce- and Yb-based heavy-fermion systems provide a beautiful example of the applicability of this theorem. de Haas-van Alphen (dHvA) experiments on a large number of Ce- and Yb-based compounds have confirmed that as long as those systems do not order magnetically, the size of the Fermi volume and FS is the large one: it always includes one full $4f$ electron or $4f$ hole, despite the number of f electrons or holes determined, e.g., from x-ray absorption spectroscopy (XAS) varying between 0 and almost one [4, 6–12, 16–18].

However, it is yet not settled at which point and how the Fermi volume and FS evolve from the large one to the small one without any $4f$ electron or hole, once these systems enter the magnetically ordered regime, where, at the end, the $4f$ electron or hole is fully localized [5]. Similarly, for the cuprate superconductors the applicability of Luttinger's theorem as well as the way how to count

* kathrin.goetze@desy.de; Present address: Deutsches Elektronen-Synchrotron (DESY), 22607 Hamburg, Germany.

† christoph.geibel@cpfs.mpg.de

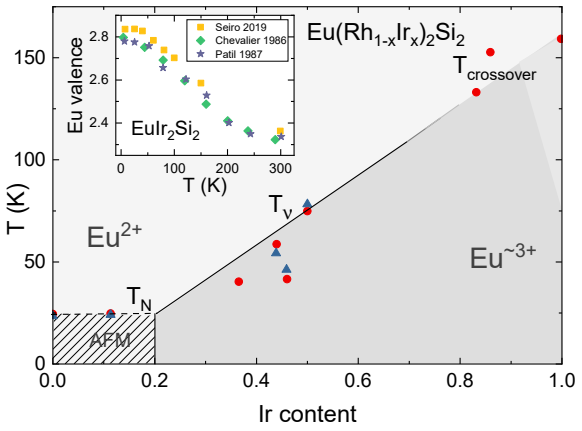

FIG. 1. Phase diagram of $Eu(Rh_{1-x}Ir_x)_2Si_2$ showing the Néel temperatures $T_N(x)$, the valence transition temperatures $T_\nu(x)$, as well as the position of the valence crossover [maximum in $\rho(T)$] observed as a function of the Ir content x: red circles from resistivity, blue triangles from susceptibility. Adapted from Ref. [24]. We add a sketch of the general phase diagram of Eu systems: dashed line: second-order paramagnetic-to-AFM phase boundary, solid line: first-order valence transition. The latter ends in a classical critical end point. Inset: Eu valence in $EuIr_2Si_2$ as a function of temperature. Data from [25–27].

the number of involved particles are yet not clear and subject of strong debates (see [19–23] and discussion and references therein). On the theoretical level, the conditions under which Luttinger's theorem should be valid is a matter of intense discussion [15].

In this context, valence-fluctuating Eu compounds present a further opportunity to study the effect of strong correlations on the FS and the applicability of Luttinger's theorem, in a situation which differs significantly from Ce- and Yb-based systems. However, because the comparatively low boiling point and high reactivity of Europium renders the crystal growth of appropriate compounds very challenging, to the best of our knowledge there is yet no report on a precise determination of the FS of a valence-fluctuating Eu system. Here, we present a dHvA study of the FS of $EuIr_2Si_2$, an archetypical valence-fluctuating Eu system. Our results indicate that the experimentally observed FS is best reproduced by band-structure calculations for a non-integer number of itinerant electrons, corresponding to an Eu valence of 2.8. This is the same valence as deduced from XAS and Mössbauer spectroscopy [25–27]. This is in contrast to the results for Ce- and Yb-based systems with a similar valence at $T = 0$, where the Fermi volume was observed to include a full $4f$ electron or hole [6]. Therefore, our present results on $EuIr_2Si_2$ put a question mark on the applicability of Luttinger's theorem in a further class of strongly correlated systems.

Europium is in the middle of the rare-earth series and can adopt any valence ν between 2 and 3, depending on chemical ligands, temperature, external pressure, and applied magnetic field. The divalent configuration has a half-filled $4f^7$ shell, where the Hund's rules result in a pure spin $S = 7/2$ angular momentum. Accordingly, Eu^{2+} shows a pronounced magnetic behavior. In contrast, trivalent Eu has a $4f^6$ shell, where Hund's rules result in the orbital $L = 3$ and the spin $S = 3$ angular momentum completely canceling to $J = L - S = 0$. Therefore, it has no stable magnetic moment and presents only Van-Vleck-type weak paramagnetism. The evolution of the properties of Eu systems as a function of chemical substitution or pressure has been widely studied [24, 28], resulting in the general phase diagram shown in Fig. 1 (shaded areas). This general phase diagram is overlaid by the results observed on the alloy $Eu(Rh_{1-x}Ir_x)_2Si_2$ [24, 29]. This allows to set the position of $EuIr_2Si_2$ within the general phase diagram.

$EuRh_2Si_2$ is representative of the situation for weak $4f$ hybridization. Such compounds show a large magnetic moment of $7\mu_B$, which orders magnetically at temperatures typically in the range 10–40 K. The observed XAS valence is 2 in the whole temperature range, and the FS corresponds to that expected for only two valence electrons for Eu [12, 27, 30]. Increasing hybridization (e.g., by substituting Ir for Rh) first results in nearly unchanged magnetic ordering temperature, without any change in other properties. However, at a given critical point, $x \approx 0.2$ in $Eu(Rh_{1-x}Ir_x)_2Si_2$, a strongly first-order transition results in an abrupt change to a magnetically non-ordered ground state with a valence typically close to 2.8. Beyond this critical point, increasing temperature leads to a strong first-order valence transition at T_ν to a paramagnetic state with a valence close to 2. Upon further increasing hybridization, T_ν increases quite strongly until a classical critical end point is reached at a temperature of about 150 K. Accordingly, for even stronger hybridization, the first-order transition is replaced by a valence crossover. Therefore, systems located slightly beyond the classical critical end point, like $EuIr_2Si_2$, show a huge decrease of the Eu valence with increasing temperature, from $\nu \approx 2.8$ at low temperatures to $\nu \approx 2.3$ at 300 K (inset of Fig 1).

This general phase diagram for Eu systems differs significantly from those for Ce- or Yb-based systems. In Ce and Yb systems, beyond a given weak hybridization, the magnetic ordering temperature decreases continuously with increasing hybridization. Thus, the magnetically ordered state usually disappears at $T = 0$ in a second-order quantum critical point [5]. The valence at and beyond this quantum critical point remains close to 3. Therefore, there is also no first-order valence transition associated with the disappearance of a magnetically ordered state. Accordingly, in the magnetically non-ordered regime Ce and Yb systems show only a weak temperature dependence of the valence, the change in ν between 0 and 300 K being typically less than 0.1 [18, 24].

Unfortunately the same denominations are used in literature for both Eu- and Ce- or Yb-based systems. For

sake of clarity, in the present paper we shall label systems with a strong temperature dependence of ν as valence-fluctuating systems, and those with a weak temperature dependence as intermediate-valent systems.

The strong temperature dependence of its valence from $\nu \approx 2.8$ at low temperatures to $\nu \approx 2.3$ at 300 K classifies $EuIr_2Si_2$ as an archetypical valence-fluctuating Eu system. The valence fluctuations are not only evident in $\nu(T)$, but also in an anomalous temperature dependence of the resistivity and of the thermal expansion, as well as a huge and strongly temperature-dependent thermopower [24, 27, 31]. Furthermore, its Sommerfeld coefficient, $\gamma = 30$ mJ/molK^2, is significantly larger than that of homologue compounds with an empty or a full f shell, $\gamma = 4.5$ mJ/molK^2 and $\gamma = 3.9$ mJ/molK^2 for $LaIr_2Si_2$ and $LuIr_2Si_2$, respectively [32]. This indicates the presence of significant correlation effects even at $T = 0$.

For zero magnetic field, ARPES measurements on $EuIr_2Si_2$ at different temperatures in combination with calculations based on density functional theory (DFT) have shown that the size and topology of the FS observed in ARPES can be well reproduced by the hole-like *spd*-derived valence band with no contribution from $4f$ electrons [33]. ARPES measurements at different temperatures revealed an increase of the size of this hole-like FS with temperature. The absolute size of this FS and its temperature dependence could be well reproduced by assuming the band filling to correspond to that expected from the Eu valence determined in XAS measurements. However, the ARPES measurements allowed to observe only part of the FS and its precise size could not be determined at low temperatures.

We have, therefore, conducted quantum-oscillation measurements on $EuIr_2Si_2$ based on the dHvA effect which are compared to DFT band-structure calculations for different Eu valences. We are, thus, not only able to establish the FS topology and effective masses but also to determine the exact contribution of a non-integer valence-electron count to the FS volume.

II. METHODS

$EuIr_2Si_2$ single crystals with a residual resistivity ratio of 100 to 140 were grown in indium flux as reported in Ref. [24].

For measuring the dHvA effect, we employed the magnetic-torque method using a capacitive cantilever in magnetic fields up to 18 T at the High Magnetic Field Laboratory (HLD-EMFL) in Dresden and in fields up to 32 T at the Laboratoire National des Champs Magnétiques Intenses (LNCMI-EMFL) in Grenoble. Both measurements were conducted at temperatures between 30 mK and 1 K in ^{3}He/^{4}He-dilution refrigerators. The respective probes were equipped with a rotator stage which allowed for angle-dependent measurements.

We performed band-structure calculations by use of the FPLO (Full Potential Local Orbital) [34] code (version 15.02) in an open-core scheme for different valence configurations. We used the local (spin) density approximation (L(S)DA) with the Perdew and Wang flavor [35]. To obtain well converged results with respect to the band dispersion, we used a regular 28 x 28 x 28 k-point mesh in the irreducible part of the Brillouin zone. The calculations were based on low-temperature lattice parameters that we determined by x-ray powder diffraction at the European Synchrotron Radiation Facility (ESRF) in Grenoble, France. We conducted calculations for the experimental value of the distance z between Eu and Si, for the optimized z value for each Eu stoichiometry, and for values in between.

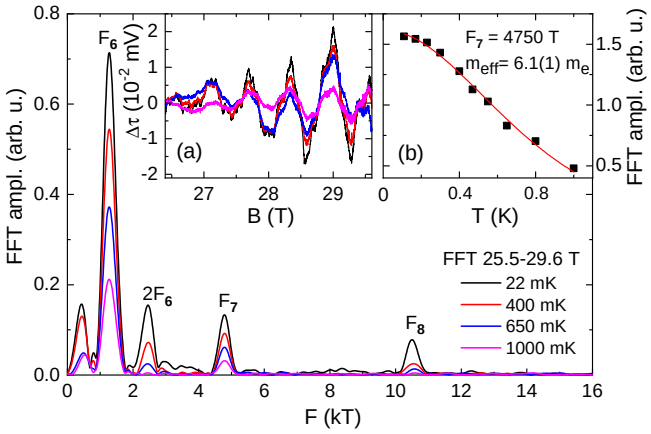

FIG. 2. Main graph: Spectral distribution of the dHvA frequencies at $\Theta_{110} = 84°$, i.e., the magnetic field is rotated by 84° from [001] to [110] of the tetragonal crystal structure, obtained by FFT based on the oscillating part of the signal shown in inset (a); black (red, blue, pink) curves measured at 22 (400, 650, 1000) mK, respectively. Inset (b): Effective mass determination for F_7 by applying the Lifshitz-Kosevich fit function (red line) to the measured FFT amplitudes.

III. RESULTS

The main part of Fig. 2 shows the result of the fast Fourier transform (FFT) of the oscillating part of the magnetic-torque signal [inset (a)] that yields the spectral distribution of the dHvA frequencies: We observe three fundamental frequencies, F_6, F_7, and F_8, at this angle. The peaks below F_6 are artifacts from the polynomial background subtraction and depend on the order of the polynomial. We display the data in inset (a) and the corresponding FFT result for different temperatures to illustrate how the amplitude of the oscillations is damped with increasing temperature. This damping effect allows us to calculate the effective masses. According to the Lifshitz-Kosevich formula the amplitude of an FFT peak is proportional to the temperature damping factor $R_T = x/\sinh x$ with $x = \alpha T m_{eff}/B$ and $\alpha \approx$

14.69 T/K [36]. The application of a fit function yields $m_{eff} = (6.1 \pm 0.1)m_e$, with m_e being the free electron mass, for frequency F_7 at $\Theta_{010} = 84°$.

We were able to resolve dHvA oscillations in the magnetic-torque signal above 10 T at the lowest temperatures at several angles for two directions of rotation. Figures 3(a) and 3(b) show the angular dependence of the experimentally obtained frequencies and compares them to the results of band-structure calculations for $Eu^{2.8+}$ and Eu^{3+}, respectively. Experimental data are plotted as black symbols. For rotation around Θ_{110} we observe three main frequencies, F_6, F_7, and F_8; all of them show an increase in frequency when rotating from $B\|[110]$ towards $B\|[001]$, with the strongest increase in F_7. For the second direction of rotation, around Θ_{010}, we observe the frequencies F_1, F_2, F_3, F_4, and F_5. F_1 hardly changes over the whole angular range which evidences that it stems from a spherical FS. F_2, F_3, and F_4 are only seen for angles close to $B\|[100]$, whereas the highest frequency for this rotation, F_5, is observed for B close to the [001] axis with little angular dependence.

In order to establish the topology of the FS of $EuIr_2Si_2$ in our experiments and the valence configuration it is based on, we have conducted band-structure calculations based on three different europium valences assuming localized $4f$ electrons. The red and green lines in Fig. 3(a) are derived from the calculated extremal cross sections for $EuIr_2Si_2$ with $Eu^{2.8+}$, which we found to show the best correspondence with our experimental data. Figure 3(d) shows calculated frequencies for trivalent europium together with the experimental results. The calculated frequencies based on the band structure with integer divalent Eu^{2+} gave a poor match with experimental data as we show in the Supplementary Information (SI) [37].

The calculations for both $Eu^{2.8+}$ and Eu^{3+} yield two bands, 48 and 49, that cross the Fermi energy and lead to two FS sheets shown for $Eu^{2.8+}$ in Figs. 3(b) and 3(c), and respectively: a star-shaped donut (band 48, green) and a more complicated, multiple-folded structure that resembles a jungle-gym (band 49, red) [37]. The most obvious difference between the calculated results for these two valence configurations is that the small FS pockets around the N point of the Brillouin zone which only occur for $Eu^{2.8+}$ explain frequency F_1 very well, whereas there are no calculated frequencies close to F_1 in the calculations based on Eu^{3+} [38]. The green line, just below F_1 close to $B\|[001]$ in Fig. 3(b), stems from the hole in the FS donut of band 48 but its curvature and limitation to angles around the [001] axis make it a poor match for F_1. Frequency spectra showing F_1 for several angles and a discussion of the band dispersion for $Eu^{2.8+}$ can be found in the SI [37].

Based on their numerical values and their angular dependences, we can further assign the calculated frequencies to the ones that were experimentally observed: As mentioned above, F_1 matches very well with the small pockets from band 49, whereas F_7 and F_8 can be at-

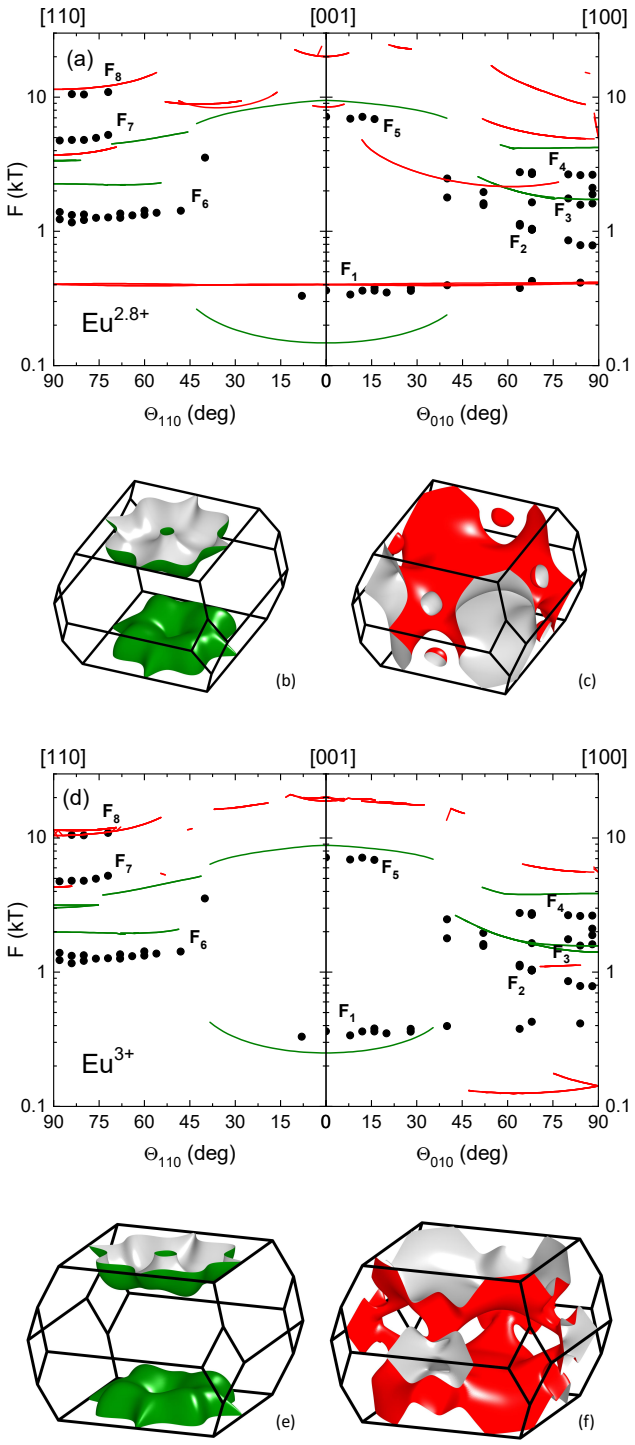

FIG. 3. (a) Angular dependence of the dHvA frequencies for $EuIr_2Si_2$. Black symbols represent experimental data whereas green and red lines are derived from the extremal FS cross sections in the result of an open-core calculation with $Eu^{2.8+}$. Green lines are based on the extremal cross-sections of the FS from band 48 shown in (b), and red lines are based on the FS from band 49 in (c). (d) Same experimental data as in (a) in comparison to calculated frequencies based on trivalent europium in $EuIr_2Si_2$. Here color coding corresponds to the depiction of the calculated FSs from band 48 in (e) and band 49 in (f).

tributed to the larger cross sections of this FS sheet. Based on the curvature of the calculated frequencies $F(\theta)$, we can assign frequencies F_2, F_4, F_5 and F_6 to orbits of the donut-shaped FS from band 48. However, we note that the calculated frequencies are consistently larger than the experimentally observed ones, and the calculated frequencies starting at about 1800 T at $B \parallel [100]$ could also be assigned to F_3. Some extremal cross sections of the jungle-gym FS with oscillation frequencies higher than 10 kT were not experimentally observed. The same is true for those frequencies stemming from the hole of the donut calculated to be of the order of 150-300 T for angles in the vicinity of $B \parallel [001]$. This could be due to very high effective masses, a high Dingle temperature, or an unfavorable curvature factor. Low frequencies can be hard to detect as quantum oscillations in this material in general start at rather high magnetic fields. If they show only a few periods in the high-field range, it is difficult to distinguish them from a polynomial magnetic background. Overall, we find good correspondence between experimental and calculated frequencies confirming that $EuIr_2Si_2$ possesses a FS corresponding to europium with valence 2.8.

We determined effective masses experimentally for three different orientations and the results, together with the respective calculated frequencies and band masses, are summarized in Table I. The quasiparticles of the donut have high effective masses between 4.8 and $11m_e$, and the jungle-gym FS shows masses of 1.4 to $11.3m_e$, when considering the complete field range between 25 and 30 T.

These quite large effective mass values are in good agreement with the enhanced zero-field Sommerfeld coefficient observed in the specific heat. The enhancement factor deduced from the ratio (measured masses)/(band masses), which reaches values up to 15, matches the ratio of about 8 between measured and calculated Sommerfeld coefficient. We note that the Sommerfeld coefficient calculated from the band structure, $\gamma_{theor} = 3.8$ mJ/molK^2, is slightly below the values observed experimentally in the non-f homologues $LaIr_2Si_2$ and $LuIr_2Si_2$ [32], as one would expect from the absence of correlation effects in the calculations. The large mass enhancement in $EuIr_2Si_2$ can be attributed to the strong correlation effects due to interaction between $4f$ and conduction electrons.

Quantum oscillations at $\Theta_{110} = 84°$ were observed over a wide field range which allowed for an investigation of the field dependence of the effective masses. The FFT of the oscillating part of the data was performed for sliding field windows of 2 to 2.5 T between 25.1 and 29.6 T for F_6 and F_7. A more detailed analysis was performed for F_8 with field windows equidistant in 1/B with $\Delta(1/B) = 0.00125$ T^{-1} and $1/B$-averaged fields B_m between 25.5 and 28.75 T. Each window comprises of 20 oscillations. The effective masses for the respective average fields B_m are shown in Fig. 4. The masses of F_6 and F_7 (inset) were found to be field independent within error bars. However, the quasiparticle mass of frequency F_8 exhibits a strong field dependence, increasing from $8.7m_e$ at $B_m = 25.5$ T to $14m_e$ at $B_m = 28.75$ T. Usually, the application of large magnetic fields leads to a suppression of electronic correlations and, therefore, a reduction of the effective masses as observed in a number of heavy-fermion compounds, such as CeB_6 [40, 41], $CeAl_2$ [42, 43], $CeRu_2Si_2$ [43], and $CeCoIn_5$ [44].

The field dependence of the effective masses is also reflected in the Dingle plot for F_8 which is discussed in the SI [37].

TABLE I. Experimental and calculated dHvA frequencies and effective masses of $EuIr_2Si_2$ for $B \parallel [001]$, $\Theta_{110} = 84°$ [39] and, $\Theta_{110} = 81.5°$. D - donut-shaped FS; J - jungle-gym FS.

	F_{exp}(kT)	$m_{eff}(m_e)$	FS	F_{calc}(kT)	$m_b(m_e)$
		$B \parallel [001]$			
F_1	0.36	1.4(6)	J	0.401	1.1
F_5	6.95	11(3)	D	8.431	2.05
		$\Theta_{110} = 84°$			
F_6	1.28	5.5(1)	D	2.254	0.36
$2F_6$	2.56	10.3(2)	-	-	-
F_7	4.75	6.1(1)	J	3.75	0.684
F_8	10.54	11.3(5)[a]	J	11.48	0.939
		$\Theta_{110} = 81.5°$			
F_6	1.17	4.8(2)	D	-	-

[a] Here, the FFT range was the complete field range for which oscillations were observed, 25 to 30 T.

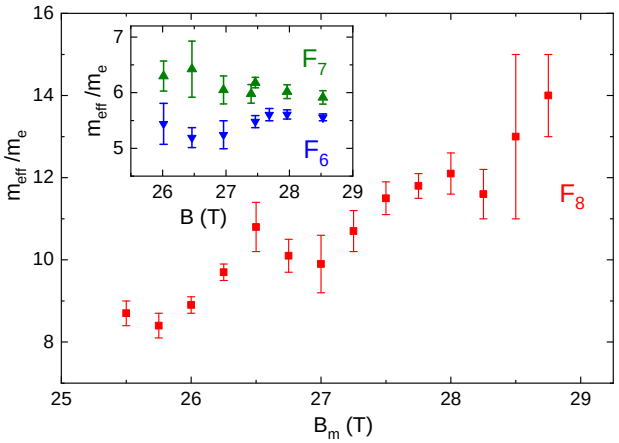

FIG. 4. Field dependence of the effective masses at $\Theta_{110} = 84°$. Main graph: effective mass of frequency F_8, inset: effective masses of F_6 and F_7.

IV. DISCUSSION

The present dHvA study on a strongly valence-fluctuation system, namely $EuIr_2Si_2$, has three main outcomes:

(1) The observed FS is best reproduced for a non-integer

number of valence electrons,

(2) the effective mass of the band carriers are enhanced by a factor of about 10 compared to the calculated band masses, and

(3) the effective mass of the heaviest band increases with magnetic field.

The observation that the experimental FS is best reproduced by band-structure calculation for a non-integer number of valence electrons corresponding to a Eu valence $\nu = 2.8$ is in agreement with the aforementioned ARPES results [33]. Their best agreement was obtained for $\nu = 2.85$ at 7 K. We note that both studies are complementary, since ARPES observed only the donut part of the FS, while our dHvA also observed the jungle-gym part. The observation of a Fermi volume with a non-integer number of electrons in a strictly stoichiometric compound with an integer number of electrons is remarkable on its own. We are not aware of a similar observation in another compound. In intermediate-valent Ce and Yb compounds, the whole $4f$ electron or $4f$ hole is included in the FS even in compounds where the valence is close to 3. Explicitly, their Fermi volume and surface is that expected for a valence of 4 (Ce) or 2 (Yb) even in the case where the XAS valence is 3.1 (Ce) or 2.9 (Yb) [6]. This is in agreement with Luttinger's theorem. When going, for example, from a Ce 3.5 to a Ce 3.1 state, the parameter which is changing within the appropriate Anderson lattice model is the strength of the hybridization between the $4f$ and conduction electrons. Since the hard form of Luttinger's theorem states that the Fermi volume is determined by the total number of interacting particles but does not depend on the strength of the interaction, one expects the Fermi volume to stay constant. Thus, the observation of a FS corresponding to a non-integer number of electrons at low temperatures in $EuIr_2Si_2$ asks for an additional mechanism [45].

There is compelling evidence that the Anderson lattice model is the appropriate theoretical model to describe Ce- and Yb-based strongly correlated metals [5, 10, 46, 47]. Its ingredients are non-$4f$ conduction electrons, a singly occupied f level far below the Fermi level, a strong on-site repulsion U_{ff} on the f level, and a hybridization V_{cf} between f and conduction electrons. Whereas the Anderson lattice model is able to explain a vast number of properties of Ce- and Yb-based Kondo lattices, it fails to reproduce the strong first-order valence transition observed in Eu systems. The presently favored and likely best approach to model systems with strong valence fluctuation and a strong first-order valence transition is to add an on-site repulsion U_{cf} between f and conduction electrons, resulting in what is commonly called extended Anderson model [48–50]. U_{cf} was originally introduced in the Falicov-Kimball model for modeling strong first-order valence transitions [51]. As the calculation of properties of this extended Anderson model is very demanding, only few results have been published on the dependence of the FS on the different parameters. They indicate significant deformation of the FS near the valence transition [52]. However, the limited amount of results do not allow for a quantitative comparison. On a general level, our result suggests that this additional U_{cf} term might require to shift from the hard Luttinger theorem to the soft Luttinger theorem, where the count of the particles in the Fermi volume has to be adjusted. A similar situation is also discussed for cuprate superconductors [22, 23]. However, there is yet no theoretical prescription how this adjustment should be done.

In our DFT band-structure calculations, the non-integer valence is achieved by assuming a static mixture between a $4f^6$ and a $4f^7$ state without any hybridization between f and other valence electrons. Therefore, there is no f-electron admixture at the FS in these DFT result. However, in reality the intermediate-valent state at low temperatures in $EuIr_2Si_2$ is not realized through a static mixture of $4f^6$ states on some sites and $4f^7$ states on the other sites, it is realized through a quantum-mechanical mixing between a $4f^6$ and a $4f^7$ state which arises due to hybridization of the f electrons with conduction electrons. Therefore, one expects some (weak) admixture of $4f$ weight into the conduction states at the Fermi level.

Going beyond the DFT level for a system with 6 or 7 localized but correlated $4f$ electrons is extremely demanding, and, to our knowledge, has yet not be done. Present calculations for the extended Anderson model are usually restricted to a single $4f$ electron. Thus, we are left with the present DFT calculations. The main effect expected from the admixture of $4f$ states is an enhancement of the effective masses. The observed enhancement by a factor of about 10 respective to the DFT masses is one order of magnitude weaker than in standard Ce- and Yb-based heavy-fermion systems, but comparable to that in intermediate-valent Ce and Yb systems far from the magnetically ordered ground state. This comparatively small mass enhancement can be understood by the much higher characteristic valence-fluctuation temperature of about 150 K, which is one order of magnitude larger than the Kondo temperature of about 10 K in typical Ce- and Yb-based heavy-fermion systems. In this type of systems, the mass enhancement scales with the inverse of the characteristic energy.

The increase of the largest effective mass with increasing magnetic field is a further clear difference between $EuIr_2Si_2$ and standard Ce- or Yb-based heavy-fermion systems. There one usually observes a decrease of m_{eff} with increasing field, because the magnetic field suppresses the Kondo effect. However, there is an obvious mechanism to explain the opposite effect in valence-fluctuating Eu systems. A magnetic field shall always stabilize the Eu^{2+} $4f^7$ state, because of its huge magnetic moment of $7\mu_B$. Indeed, in valence-fluctuating Eu systems located in the regime where one observes a temperature-induced first-order valence transition, such as in $Eu(Rh_{1-x}Ir_x)_2Si_2$ in the range $0.2 < x < 0.6$, application of a magnetic field at low temperatures also results in a strong first-order transition to a magnetic divalent Eu state, in full analogy with the effect of in-

creasing temperature [29, 53]. Reason for this analogy is the large moment (magnetic field) and the large magnetic entropy (temperature) of the $4f^7$ state. Accordingly, for systems beyond the classical critical end point, such as $EuIr_2Si_2$, the field-induced first-order valence transition evolves into a field-induced valence crossover. In such systems the temperature dependence of the resistivity indicates that from low temperatures on, the valence fluctuations first increase with temperature, exhibit a broad maximum, and decrease again at high temperature.

According to the analogy between magnetic field and temperature, applying a magnetic field should first increase the valence fluctuations; hence, one expects a related increase of the effective masses. Using scaling between specific heat and magnetic field, one can estimate the maximum in the fluctuations to be in the range 100–150 T in $EuIr_2Si_2$. Therefore, it is not surprising to see an enhancement of the effective masses in the range 25–30 T. On the other hand, we did not observe a change in the size of the FS. Thus, increasing valence fluctuations first enhance the effective masses before they affect the size of the FS.

A last noticeable point: The Dingle temperatures we deduced from the field dependence of our dHvA oscillations are comparatively high, 3.7 K and 7.9 K, see [37]. This implies that in $EuIr_2Si_2$ impurities cause strong scattering of quasiparticles despite the high RRR value of 100–140 [24]. This is reminiscent of the strong enhancement of the residual resistivity observed in the vicinity of the quantum critical point in Ce- or Yb-based systems [5]. A likely reason is that a defect on the Ir or the Si site shall not only produce its own scattering, but shall affect the nearest-neighbor Eu sites, changing their valence and thus partially destroying the coherence in the Eu lattice.

V. SUMMARY AND OUTLOOK

We present a study of the FS and of the effective masses in the valence-fluctuating compound $EuIr_2Si_2$ based on dHvA measurements and corresponding band-structure calculations. We observed quite a number of quantum oscillations in a wide range of directions. In order to analyze these experimental results, we performed DFT-based band-structure calculations within an open core approach assuming different values for the mean Eu valence ν. The best fit between observed and calculated frequencies was obtained for $\nu = 2.8$, in agreement with previous ARPES results. Although $\nu = 2.8$ corresponds to the valence determined with XAS, this result is quite surprising. The Luttinger theorem relevant for such strongly correlated electron systems states that the Fermi volume includes the whole f-degree of freedom, independent of the Eu valence. Therefore, the FS was expected to correspond to that of a fully trivalent Eu state, as observed in Ce- and Yb-based strongly correlated systems. The observation of a Fermi volume with a noninteger number of electrons in a strictly stoichiometric compound is a remarkable observation on its own. This result suggests that the additional on-site repulsion between f and conduction electrons U_{cf}, which has to be introduced to model valence-fluctuating Eu systems, requires a shift from the hard to the soft Luttinger theorem, where the count of the particles in the Fermi volume has to be adjusted. Such a shift and adjustment is also discussed for cuprate superconductors.

On a general level, the present results and the ARPES results on $EuIr_2Si_2$ of Ref. [33] indicate that in strongly valence-fluctuating Eu-based systems the size of the Fermi surface is directly proportional to the bulk valence. In contrast, in Ce-and Yb-based systems with a weak temperature dependence of the bulk valence, both properties are completely disconnected: in these systems preliminary results indicate a huge change in the Fermi volume, with one f degree of freedom disappearing between the lowest temperature and room temperature [54], while the bulk valence changes only by a few percent [18].

The strong electronic correlations due to valence fluctuations and hybridization between f and conduction electrons result in an enhancement of the effective mass of the conduction electrons. From the temperature dependence of the oscillations we deduced an enhancement factor of about 10 respective to the band masses. This is in agreement with the enhancement deduced from the Sommerfeld coefficient and in accordance with the characteristic temperature scale of the valence fluctuations in $EuIr_2Si_2$. Interestingly, we observed the largest mass to increase even further with increasing magnetic field. This can be attributed to an enhancement of valence fluctuations connected to the valence crossover expected at much higher magnetic field. In the future, it would be interesting to follow the evolution of the FS and of the effective masses across the expected field-induced valence crossover. However, this requires measurements in fields up to the order of 100 T.

Our to some extend surprising results point to the relevance of valence-fluctuating Eu system for the understanding of FS and Fermi volume in strongly correlated systems, and ask for further similar studies in other valence-fluctuating Eu compounds. Unfortunately, the crystal growth of the archetypical valence-fluctuating compounds $EuCu_2Si_2$ and $EuPd_2Si_2$ are plagued by stoichiometry problems resulting in much too high residual resistivities. Our attempts on the compound $EuNi_2P_2$ also failed to observe quantum oscillations, likely because of a still too high residual resistivity. Thus, it might be necessary to find new valence-fluctuating Eu systems appropriate for such a task.

ACKNOWLEDGMENTS

We acknowledge support from the DFG through the Würzburg-Dresden Cluster of Excellence on Complexity and Topology in Quantum Matter – *ct.qmat* (EXC 2147, Project No. 390858490), the ANR-DFG grant 'Fermi-

NESt' including the DFG Grant GE 602/4-1, and by HLD at HZDR and LNCMI-CNRS, which are both members of the European Magnetic Field Laboratory (EMFL). Work performed at the University of Warwick is supported by the European Research Council (ERC) under the European Union's Horizon 2020 research and innovation program (Grant Agreement No. 681260). K.G. and I.K. acknowledge support from the DFG within GRK1621.

[1] B. Vignolle, D. Vignolles, D. LeBoeuf, S. Lepault, B. Ramshaw, R. Liang, D. A. Bonn, W. N. Hardy, N. Doiron-Leyraud, A. Carrington, N. E. Hussey, L. Taillefer, and C. Proust, C. R. Phys. **12**, 446 (2011).
[2] S. E. Sebastian, N. Harrison, and G. G. Lonzarich, Rep. Prog. Phys. **75**, 102501 (2012).
[3] B. Keimer, S. A. Kivelson, M. R. Norman, S. Uchida, and J. Zaanen, Nature **518**, 179 (2015).
[4] G. Zwicknagl, Adv. Phys. **41**, 203 (1992).
[5] H. v. Löhneysen, A. Rosch, M. Vojta, and P. Wölfle, Rev. Mod. Phys. **79**, 1015 (2007).
[6] Y. Ōnuki and R. Settai, Low Temp. Phys. **38**, 89 (2012).
[7] J. D. Denlinger, G. H. Gweon, J. W. Allen, C. G. Olson, M. B. Maple, J. L. Sarrao, P. E. Armstrong, Z. Fisk, and H. Yamagami, J. Electron Spectros. Relat. Phenomena Strongly correlated systems, **117-118**, 347 (2001).
[8] T. Okane, T. Ohkochi, Y. Takeda, S.-i. Fujimori, A. Yasui, Y. Saitoh, H. Yamagami, A. Fujimori, Y. Matsumoto, M. Sugi, N. Kimura, T. Komatsubara, and H. Aoki, Phys. Rev. Lett. **102**, 216401 (2009).
[9] K. Kummer, S. Patil, A. Chikina, M. Gttler, M. Hppner, A. Generalov, S. Danzenbcher, S. Seiro, A. Hannaske, C. Krellner, Y. Kucherenko, M. Shi, M. Radovic, E. Rienks, G. Zwicknagl, K. Matho, J. Allen, C. Laubschat, C. Geibel, and D. Vyalikh, Phys. Rev. X **5**, 011028 (2015).
[10] S. Jang, J. D. Denlinger, J. W. Allen, V. S. Zapf, M. B. Maple, J. N. Kim, B. G. Jang, and J. H. Shim, Proc. Natl. Acad. Sci. U.S.A. **117**, 23467 (2020).
[11] M. Gttler, K. Kummer, K. Kliemt, C. Krellner, S. Seiro, C. Geibel, C. Laubschat, Y. Kubo, Y. Sakurai, D. V. Vyalikh, and A. Koizumi, Phys. Rev. B **103**, 115126 (2021).
[12] M. Gttler, A. Generalov, S. I. Fujimori, K. Kummer, A. Chikina, S. Seiro, S. Danzenbcher, Y. M. Koroteev, E. V. Chulkov, M. Radovic, M. Shi, N. C. Plumb, C. Laubschat, J. W. Allen, C. Krellner, C. Geibel, and D. V. Vyalikh, Nat. Commun. **10**, 796 (2019).
[13] K. Andres, J. E. Graebner, and H. R. Ott, Phys. Rev. Lett. **35**, 1779 (1975).
[14] J. M. Luttinger, Phys. Rev. **119**, 1153 (1960).
[15] J. T. Heath and K. S. Bedell, New J. Phys. **22**, 063011 (2020).
[16] S. Araki, R. Settai, T. C. Kobayashi, H. Harima, and Y. Ōnuki, Phys. Rev. B **64**, 224417 (2001).
[17] P. M. C. Rourke, A. McCollam, G. Lapertot, G. Knebel, J. Flouquet, and S. R. Julian, J. Phys.: Conf. Ser. **150**, 042165 (2009).
[18] K. Kummer, C. Geibel, C. Krellner, G. Zwicknagl, C. Laubschat, N. B. Brookes, and D. V. Vyalikh, Nat. Commun. **9**, 2011 (2018).
[19] K. B. Dave, P. W. Phillips, and C. L. Kane, Phys. Rev. Lett. **110**, 090403 (2013).
[20] M. S. Hossain, M. Mueed, M. Ma, K. Villegas Rosales, Y. Chung, L. Pfeiffer, K. West, K. Baldwin, and M. Shayegan, Phys. Rev. Lett. **125**, 046601 (2020).
[21] E. Kozik, M. Ferrero, and A. Georges, Phys. Rev. Lett. **114**, 156402 (2015).
[22] C. Proust and L. Taillefer, Annu. Rev. Condens. Matter Phys. **10**, 409 (2019).
[23] S. Sachdev, Rep. Prog. Phys. **82**, 014001 (2018).
[24] S. Seiro and C. Geibel, J. Phys.: Condens. Matter **23**, 375601 (2011).
[25] B. Chevalier, J. M. D. Coey, B. Lloret, and J. Etourneau, J. Phys. C: Solid State Phys. **19**, 4521 (1986).
[26] S. Patil, R. Nagarajan, L. C. Gupta, R. Vijayaraghavan, and B. D. Padalia, Solid State Commun. **63**, 955 (1987).
[27] S. Seiro, Y. Prots, K. Kummer, H. Rosner, R. C. Gil, and C. Geibel, J. Phys.: Condens. Matter **31**, 305602 (2019).
[28] Y. Ōnuki, M. Hedo, and F. Honda, J. Phys. Soc. Japan **89**, 102001 (2020).
[29] A. Mitsuda, T. Fujimoto, E. Kishaba, S. Hamano, A. Kondo, K. Kindo, and H. Wada, J. Phys. Soc. Jpn. **85**, 124703 (2016).
[30] K. Götze *et al.*, *unpublished*.
[31] U. Stockert, S. Seiro, N. Caroca-Canales, E. Hassinger, and C. Geibel, Phys. Rev. B **101**, 235106 (2020).
[32] C. Krellner, Dissertation, TU Dresden (2009).
[33] S. Schulz, I. A. Nechaev, M. Gttler, G. Poelchen, A. Generalov, S. Danzenbcher, A. Chikina, S. Seiro, K. Kliemt, A. Y. Vyazovskaya, T. K. Kim, P. Dudin, E. V. Chulkov, C. Laubschat, E. E. Krasovskii, C. Geibel, C. Krellner, K. Kummer, and D. V. Vyalikh, npj Quantum Materials **4**, 26 (2019).
[34] K. Koepernik and H. Eschrig, Phys. Rev. B **59**, 1743 (1999).
[35] J. P. Perdew and Y. Wang, Phys. Rev. B **45**, 13244 (1992).
[36] D. Shoenberg, *Magnetic Oscillations in Metals* (Cambridge University Press, Cambridge, England, 1984).
[37] See Supplementary Information for calculated dHvA frequencies for $EuIr_2Si_2$ with divalent europium, examples of FFTs showing frequency F_1 for several angles, a depiction of the band dispersion close to the Fermi energy, and Dingle plots for F_6, F_7, and F_8.
[38] The calculated frequencies shown in Fig. 3(a) are determined using a z value of 0.3754. We have also conducted calculations using the measured value of z, 0.3731, which leads to an underestimation of the size of the N point pockets, and for the optimized value, 0.3768, which leads to an overestimation of the size of these pockets. $z = 0.3754$ gives the best correspondence with the experimental values of frequency F_1. We stress, however, that the small pockets occur for all those z values for $Eu^{2.8+}$, but not for calculations using divalent Eu^{2+} or trivalent Eu^{3+}.

[39] For $\Theta_{110} = 84°$, the complete range field range for which oscillations were observed were used. The error bars in Fig. 4 are bigger because of the smaller field ranges.

[40] W. Joss, J. M. van Ruitenbeek, G. W. Crabtree, J. L. Tholence, A. P. J. van Deursen, and Z. Fisk, Phys. Rev. Lett. **59**, 1609 (1987).

[41] N. Harrison, P. Meeson, P.-A. Probst, and M. Springford, J. Phys.: Condens. Matter **5**, 7435 (1993).

[42] E. G. Haanappel, L. Pricopi, A. Demuer, and P. Lejay, Physica B **259-261**, 1081 (1999).

[43] L. Pricopi, E. G. Haanappel, S. Asknazy, N. Harrison, M. Bennett, P. Lejay, A. Demuer, and G. Lapertot, Physica B **294-295**, 276 (2001).

[44] R. Settai, H. Shishido, S. Ikeda, Y. Murakawa, M. Nakashima, D. Aoki, Y. Haga, H. Harima, and Y. Ōnuki, J. Phys.: Condens. Matter **13**, L627 (2001).

[45] Eu systems have the additional problem that they do not switch from 1 to zero electrons or holes as Ce or Yb, respectively, but from 6 to 7 f electrons. However, in a first approximation that can be considered as one f degree of freedom, i.e., one f electron as in Ce or Yb systems.

[46] V. Zlati and R. Monnier, Phys. Rev. B **71**, 165109 (2005).

[47] H. Pfau, R. Daou, S. Lausberg, H. R. Naren, M. Brando, S. Friedemann, S. Wirth, T. Westerkamp, U. Stockert, P. Gegenwart, C. Krellner, C. Geibel, G. Zwicknagl, and F. Steglich, Phys. Rev. Lett. **110**, 256403 (2013).

[48] Y. Onishi and K. Miyake, Physica B **281-282**, 191 (2000).

[49] Y. Saiga, T. Sugibayashi, and D. S. Hirashima, J. Phys. Soc. Japan **77**, 114710 (2008).

[50] K. Kubo, J. Phys. Soc. Japan **80**, 114711 (2011).

[51] L. M. Falicov and J. C. Kimball, Phys. Rev. Lett. **22**, 997 (1969).

[52] T. Sugibayashi and H. Kusunose, J. Phys.: Conf. Ser. **273**, 012057 (2011).

[53] H. Yasumura, Y. Narumi, T. Nakamura, Y. Kotani, A. Yasui, E. Kishaba, A. Mitsuda, H. Wada, K. Kindo, and H. Nojiri, J. Phys. Soc. Jpn. **86**, 054706 (2017).

[54] S. Y. Agustsson, S. V. Chernov, K. Medjanik, S. Babenkov, O. Fedchenko, D. Vasilyev, C. Schlueter, A. Gloskovskii, Y. Matveyev, K. Kliemt, C. Krellner, J. Demsar, G. Schönhense, and H.-J. Elmers, Journal of Physics: Condensed Matter **33**, 205601 (2021).

Supplemental Information to Fermi Surface of a System with Strong Valence Fluctuations: Evidence for a Non-Integer Count of Valence Electrons in $EuIr_2Si_2$

K. Götze,[1,2,*] B. Bergk,[1,3] O. Ignatchik,[1] A. Polyakov,[1] I. Kraft,[4,5] V. Lorenz,[6] H. Rosner,[4] T. Förster,[1] S. Seiro,[4,6] I. Sheikin,[7] J. Wosnitza,[1,5] and C. Geibel[4,†]

[1] *Hochfeld-Magnetlabor Dresden (HLD-EMFL) and Würzburg-Dresden Cluster of Excellence ct.qmat, Helmholtz-Zentrum Dresden-Rossendorf, 01328 Dresden, Germany*

[2] *Department of Physics, University of Warwick, Coventry, CV4 7AL, United Kingdom*

[3] *Institut für Werkstoffwissenschaft, TU Dresden, 01062 Dresden, Germany*

[4] *Max Planck Institute for Chemical Physics of Solids, 01187 Dresden, Germany*

[5] *Institut für Festkörper- und Materialphysik, Technische Universität Dresden, 01062 Dresden, Germany*

[6] *Leibniz IFW Dresden, 01069 Dresden, Germany*

[7] *Laboratoire National des Champs Magnétiques Intenses (LNCMI-EMFL), CNRS, UGA, 38042 Grenoble, France*

(Dated: March 23, 2022)

* kathrin.goetze@desy.de; Present address: Deutsches Elektronen-Synchrotron (DESY), 22607 Hamburg, Germany.

† christoph.geibel@cpfs.mpg.de

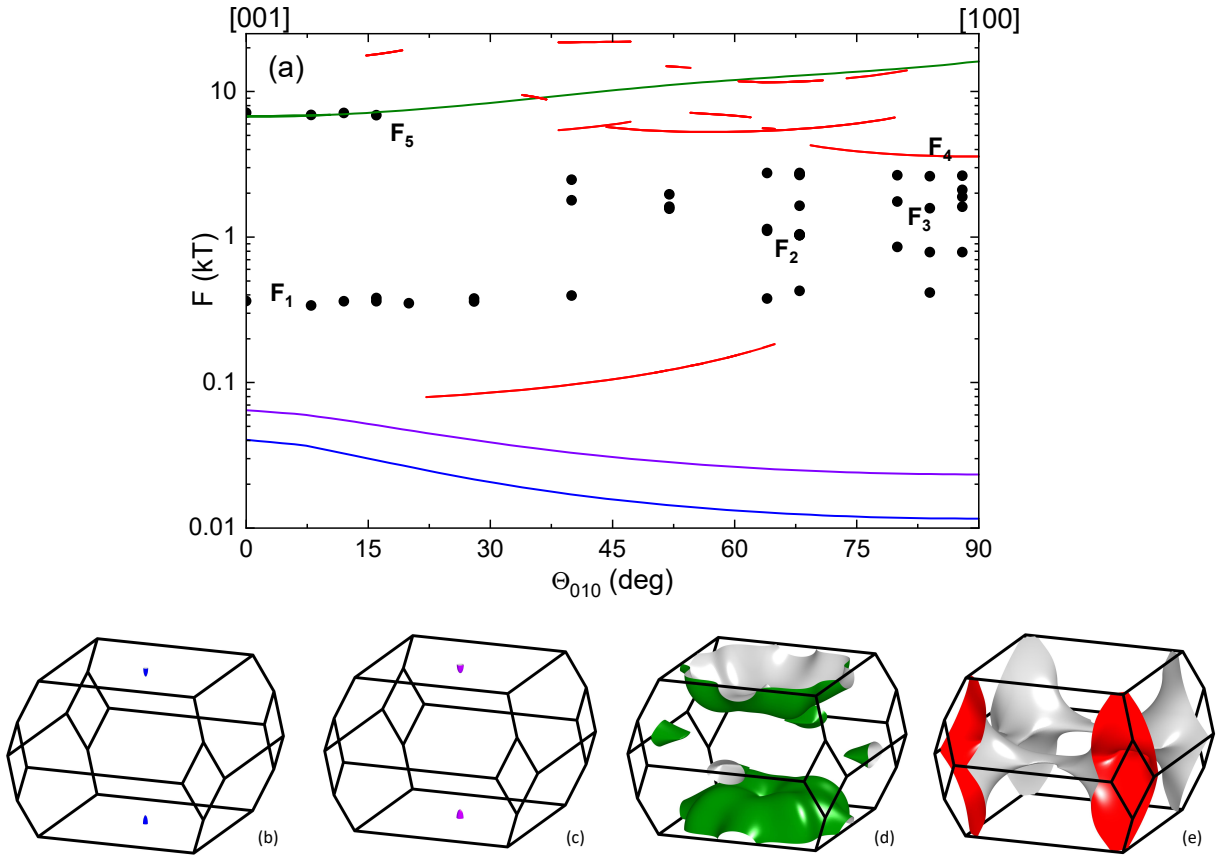

FIG. S1. (a) Comparison of experimental data (black symbols) and calculated frequencies (red, green, blue, and purple lines) obtained from band-structure calculations for divalent europium. Color coding corresponds to the depiction of the calculated FSs from band 46 in (b), band 47 in (c), band 48 in (d), and band 49 in (e)

A. Calculated dHvA frequencies and FSs for divalent Eu

Figure S1(a) shows the quantum-oscillation frequencies derived from the theoretically determined FSs (Figs. S1(b)–(e)) for divalent Eu in $EuIr_2Si_2$. The comparison to our experimental data (black symbols) shows that there is hardly any correspondence. As shown and discussed in the main text, the calculations for $Eu^{2.8+}$ give the best agreement between experiment and calculation.

B. Frequency F_1 and small Fermi surface pockets in calculations based on $Eu^{2.8+}$

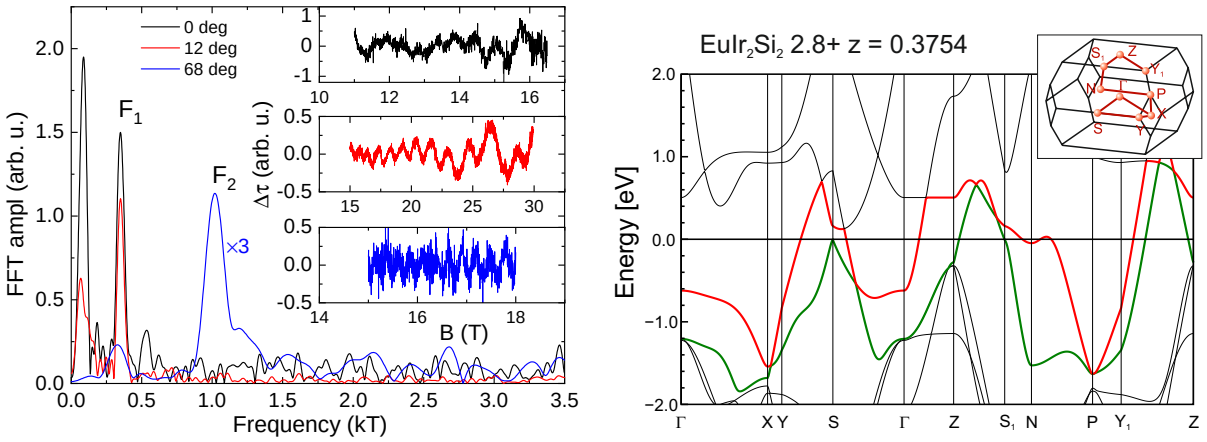

(a) (b)

FIG. S2. (a) Frequency spectrum obtained by FFT of the oscillating part of the torque signal after background subtraction (shown in the insets) for $\Theta_{010} = 0°, 12°, 68°$. (b) Band dispersion along the high-symmetry axes of $EuIr_2Si_2$ for $Eu^{2.8+}$ with $z = 0.3754$. Inset: Brillouin zone and its symmetry points.

In Fig. S2 (a), we show examples of frequency spectra focusing on the low frequency F_1. These data were measured upon rotation from $B\|[001]$ to $B\|[100]$. The black and red curves (measured at 0 and 12°, respectively) both show a clear peak at 350 T. For $\Theta_{010} = 68°$ (blue), the spectrum is dominated by the higher frequency F_2 but nevertheless there is a distinct peak at 330 T. The insets of Fig. S2 (a) show the oscillating part of the data just mentioned.

The band dispersion for $EuIr_2Si_2$ with $Eu^{2.8+}$ is shown in Fig. S2 (b) with band 48 highlighted in green and band 49 in red. Band 49 crosses the Fermi energy within a very small energy range between S1 and N, and between N and P leading to the small FS pockets, shown in Fig. 3(d) of the main text, which are the origin of the quantum oscillations with frequency F_1. The high-symmetry points of the Brillouin zone are annotated in the inset of Fig. S2 (b).

C. Dingle temperature

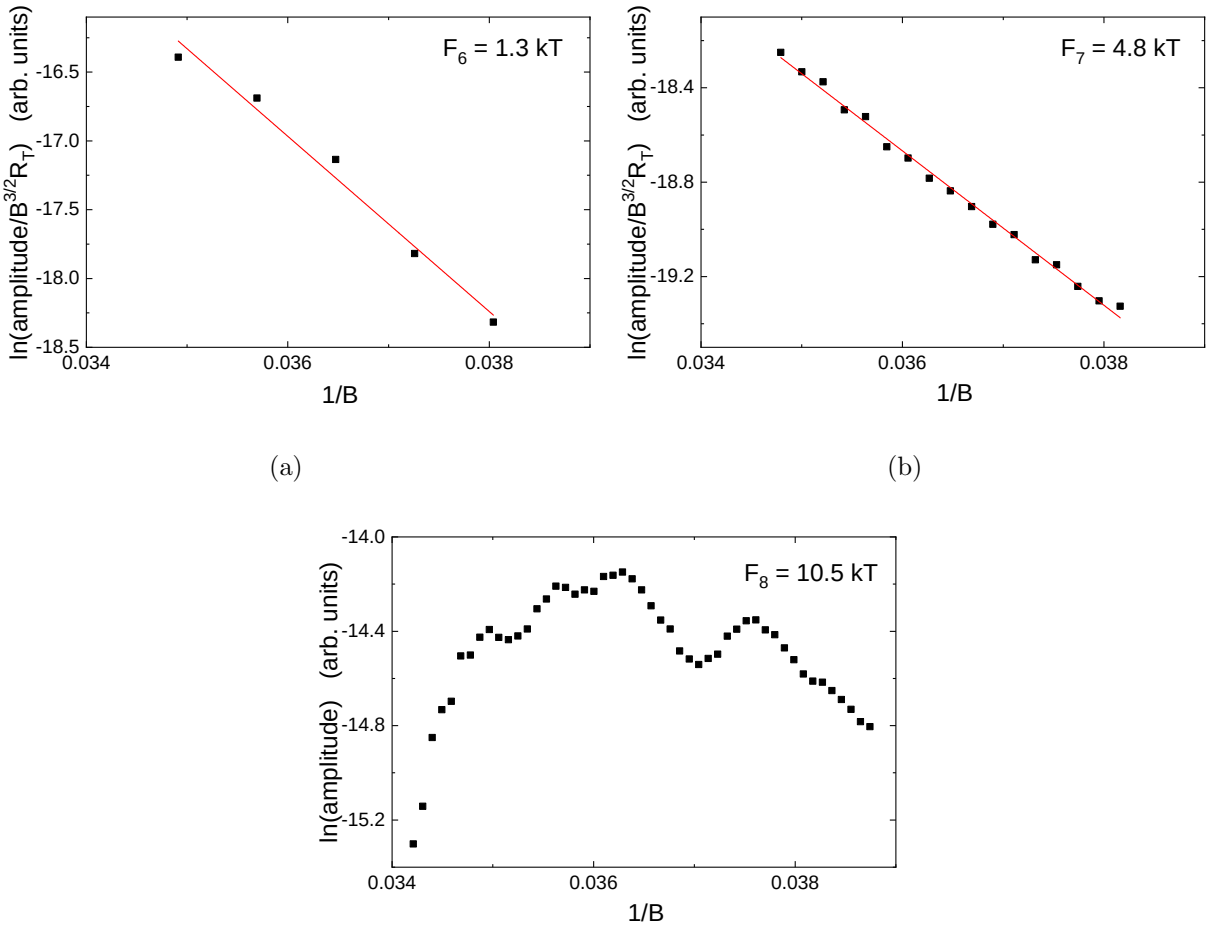

FIG. S3. Inverse field dependence of the FFT amplitudes shown as Dingle plots for frequencies F_6 (a) and F_7 (b) including linear fits, and of the logarithm of the FFT amplitudes for frequency F_8 (c), all at $\Theta_{110} = 84°$ and 70 mK. The Dingle temperatures for F_6 and F_7 are 7.9 K and 3.7 K, respectively. FFTs were performed over four oscillation periods for each data point.

The field dependence of the quantum-oscillation amplitudes measured by the torque technique can be described by

$$A \propto R_T R_D B^{3/2},$$

with amplitude A, temperature damping factor R_T, and Dingle factor R_D [S1]. The Dingle factor $R_D = \exp(-\alpha m_b T_D/B)$ ($\alpha \approx 14.69$ T/K) depends on the band mass m_b and the Dingle temperature which is inversely proportional to the scattering rate τ by $T_D = \hbar/(2\pi k_B \tau)$.

The Dingle temperature is, therefore, a measure for sample quality. So-called Dingle plots as shown in Figs. S3 (a) and S3 (b) for F_6 and F_7 display the amplitude of the dHvA oscillations of a certain frequency as $\ln(A/[R_T B^{3/2}])$ vs $1/B$. The Dingle temperature can then be determined from the slope of a linear fit to the data [S2]. The dHvA amplitudes in the Dingle plots of F_6 and F_7 show the expected linear dependence, while those of F_8 (here shown as the logarithm of the amplitude of the dHvA frequencies) deviate clearly from linearity and decrease strongly for high fields indicating additional scattering mechanisms.

[S1] D. Shoenberg, *Magnetic Oscillations in Metals* (Cambridge University Press, Cambridge, 1984).

[S2] For the determination of the Dingle temperature from the slope of the linear fits we have replaced the band mass m_b by the effective mass m_{eff}, which has been determined from the temperature-dependent decrease of the amplitudes.